THE DIRECT POTENTIAL METHOD IN
THREE DIMENSIONAL ELASTOSTATICS

T. A. Cruse

Report SM-13

June 1968

Department of Mechanical Engineering
Carnegie Institute of Technology
Carnegie-Mellon University
Pittsburgh, Pennsylvania

THE DIRECT POTENTIAL METHOD IN THREE-DIMENSIONAL ELASTOSTATICS

I. Introduction

The analysis of the stresses and displacements in an elastic body due to some state of loading and confinement usually begins with assumptions which reduce the dimension of the field equations. In many complex problems this reduction is from three dimensions to the familiar two dimensional representations of plane stress and plane strain. The reduction to two dimensions is made so that the problem becomes tractable and the reduction may be justified by the state of loading and the geometrical configuration of the body. For example, in the investigation of the stress field in the vicinity of a crack through a thick body one may consider the region far from the surfaces of the body to be in a state of plane strain. On the other hand, near the surface the stress field is more nearly in a state of plane stress. The crucial problem at this point is in determining just when one model or the other may be applied and whether these two models include all important features of the stress field. In some other cases the reduction to one or two dimensions may be made by conditions of symmetry such as when the stresses satisfy the condition of polar symmetry and in yet other cases the reduction to one or two dimensions may be made solely on the basis of the need for some estimate of the stress state.

The second crucial aspect of the analysis involves the shape and connectivity of the region. If the region has a simple shape for the dimension of the problem, e.g., the rectangle, the circle, the half-space, etc., it is likely that well documented analytic procedures

are available such as separation of variables (or the related use of transforms). If the shape is complex, as in the case of many real problems, one is forced to adopt some degree of approximation with related numerical procedures. Some problems may be made tractable by replacing the actual shape by an ideal shape as in the analysis of elliptic or parabolic shaped cracks and notches. In the case of the most general shapes of regions solutions may not yet be established and those problems that have been solved have been attacked by entirely numerical methods such as finite differences or finite elements.

While the need for numerical procedures for complex shapes is obvious and will not change, the restriction to two dimensional representations is dictated by the present state of knowledge of solution methods. Therefore, there is a need for new procedures of analysis which can be extended to analysis in three dimensions. These new procedures are necessary to refine the analysis of some problems solved with two dimensional assumptions as well as to analyze previously intractable problems. In keeping with the spirit of true three dimensional analysis the solution method should maintain the highest state of generality as to geometry, connectivity and loading, as possible.

A method offering the broadest capabilities and ease of use is the direct potential method. This solution procedure has been successfully applied to two dimensional problems in elastostatics [1] and transient elastodynamics [2] and [3]. It is the purpose of this paper to extend the capability to problems of three dimensional elastostatics.

The potential methods of solution in elasticity closely parallel the classical solution methods [4] for Laplace's equation collectively called potential theory. The recent revival of the potential formulation method is due both to the use of a boundary identity analogous to Green's boundary identity in potential theory [5] and also to the capability of solving large systems of algebraic equations with the digital computer. The singular feature of the potential method for boundary and initial value problems is the capability of obtaining solution forms which automatically include the prescribed data, boundary configuration, and region connectivity. The potential method may be divided into two approaches: the indirect and the direct potential methods.

In the indirect procedure integral equations are written in terms of harmonic functions from which the displacements and stresses must be derived by differentiation. The necessary boundary values for these functions must be established by integration of the actual boundary conditions. The indirect method has been applied to the problem of vibrations of an elastic body [6] and to problems in acoustics.

The direct method described in [1] and [2] obtains integral equations whose unknowns are the unknown surface tractions and displacements, thus eliminating the need for intermediate potential functions. The interior stresses and displacements are calculated directly from tensor and vector identities respectively. Numerical solution of the integral equations is achieved by a reduction to algebraic equations and solution of the algebraic equations by standard digital computer methods.

The direct potential method has two advantages over other approximate methods: the dimension of the problem is reduced by one, and all numerical approximations take place at the surface of the body. Further, the formulation of the integral equations and their reduction to algebraic equations is not restricted by geometric considerations. The formulation and subsequent solution offer to the analyst the utmost in generality and applicability to nontrivial problems and the procedures have been fully automated.

2. Integral Equation Formulation

The analysis in this paper is restricted to the analysis of classical elastostatic problems for which the material may be taken as isotropic and homogeneous. The usual Navier equations of equilibrium in the absence of body forces is given by

$$(\lambda + \mu)u_{i,ij} + \mu u_{j,ii} = 0 \qquad (i,j = 1,2,3) \qquad (2.1)$$

for the displacement vector, $u_i(X)$. The solution to this differential equation must also satisfy appropriate boundary conditions on the displacements and tractions, respectively given as

$$u_i(X) = q_i \qquad , X \varepsilon S_{(u_i)}$$

and $\qquad\qquad\qquad\qquad\qquad\qquad\qquad\qquad\qquad\qquad$ (2.2)

$$t_i(X) = \sigma_{ij}n_j = p_i , X \varepsilon S_{(t_i)} .$$

The unit vector n_i is the *outward* normal vector for the body R. The stress components, σ_{ij}, and displacement gradients are related by Hooke's law

$$\sigma_{ij} = \lambda \delta_{ij} u_{m,m} + \mu(u_{i,j} + u_{j,i}). \qquad (2.3)$$

The well-known solution to Kelvin's problem (a concentrated unit load in the infinite body) is given by the tensor field, [7],

$$U_{ij} = \frac{1}{4\pi\mu} (\frac{1}{r}) [\frac{3 - 4\nu}{4(1 - \nu)} \delta_{ij} + \frac{1}{4(1 - \nu)} r_{,i} r_{,j}], \qquad (2.4)$$

for displacements in the x_j directions due to point loads in each of the x_i directions. These displacement components are given by the operation

$$u_j = U_{ij} e_i \qquad (2.5)$$

on the base vectors, e_i. The distance between the field point X and the load point ξ is given by

$$r = [(x_i - \xi_i)(x_i - \xi_i)]^{1/2}. \qquad (2.6)$$

The traction vectors, $t_j = T_{ij} e_i$, are determined from Eq. (2.4) and are given by the tensor components, [7],

$$T_{ij} = - \frac{k}{4\pi} (\frac{1}{r^2}) [\frac{\partial r}{\partial n} (\delta_{ij} + \frac{3}{1 - 2\nu} r_{,i} r_{,j}) - n_j r_{,i} + n_i r_{,j}], \qquad (2.7)$$

where $k = \dfrac{1 - 2v}{2(1 - v)}$.

Now letting the load point ξ be surrounded by a small spherical region, R^*, with the surface, Γ, Betti's third identity may be written as

$$\int\limits_{S+\Gamma} (u_i T_{ji} - t_i U_{ji})dS = 0, \qquad (2.8)$$

where u_i, t_i are the displacements and tractions for the unknown stress state. By taking the limits for $R^* \to 0$ in the usual way (see [2]) the following identity results

$$u_j(\xi) = - \int\limits_{S} u_i(X)T_{ji}(X,\xi)dS(X)$$

$$\qquad (2.9)$$

$$+ \int\limits_{S} t_i(X)U_{ji}(X,\xi)dS(X).$$

This is Somigliana's identity for the displacements inside the body, R, due to known surface tractions and displacements. The interior stress state may be generated from Eq. (2.9) by differentiation and is given by

$$\sigma_{ij}(\xi) = - \int\limits_{S} u_k(X)S_{kij}(X,\xi)dS(X)$$

$$\qquad (2.10)$$

$$+ \int\limits_{S} t_k(X)D_{kij}(X,\xi)dS(X).$$

By utilizing the identity

$$\frac{\partial r}{\partial x_i} = - \frac{\partial r}{\partial \xi_i} \qquad (2.11)$$

the tensors D_{kij} and S_{kij} are found to be

$$D_{kij} = \frac{k}{4\pi} (\frac{1}{r^2})(\delta_{ki} r,_j + \delta_{kj} r,_i - \delta_{ij} r,_k + \frac{3}{1 - 2\nu} r,_i r,_j r,_k) \qquad (2.12)$$

and

$$S_{kij} = \frac{k\mu}{4\pi} (\frac{2}{r^3})\{3 \frac{\partial r}{\partial n} [\delta_{ij} r,_k + \frac{\nu}{1 - 2\nu} (\delta_{ki} r,_j + \delta_{kj} r,_i)$$

$$- \frac{5}{1 - 2\nu} r,_i r,_j r,_k] + \frac{3\nu}{1 - 2\nu} (n_i r,_j r,_k + n_j r,_i r,_k) \qquad (2.13)$$

$$+ 3n_k r,_i r,_j + n_j \delta_{ki} + n_i \delta_{kj} - \frac{1 - 4\nu}{1 - 2\nu} n_k \delta_{ij}\}.$$

The comma-differentiation is with respect to X, the integration point in Eq. (2.10).

Since it is not possible to independently specify corresponding components of the displacements and the tractions at a boundary point Eq. (2.9) is not suitable for the solution of the given problem. Let two points on the surface be given by P and Q and let Q represent the variable point X. Let the point p be the point ξ inside R. Finally, allow the field point p approach the boundary point P. From the continuity of $u_i(\xi)$ and by the usual methods of potential theory [4] the following equation results

$$\frac{1}{2} u_j(P) + \int_S u_i(Q) T_{ji}(Q,P) dS(Q)$$

$$(2.14)$$

$$= \int_S t_i(Q) U_{ji}(Q,P) dS(Q).$$

The integrals are to be interpreted in the sense of the Cauchy Principal Value. This is the usual boundary constraint equation between the surface tractions and surface displacements. When the boundary conditions, Eq. (2.2), are applied Eq. (2.14) becomes sets of singular integral equations for the unknown boundary quantities. The numerical solution of these equations is discussed in the next section.

3. Numerical Solution of the Integral Equations

General analytic solutions to the integral equations (2.14) are not available and it is therefore necessary to solve the equations numerically. The integral equations reduce to algebraic equations by discretizing the boundary data. Following the procedure used previously in acoustics [8] the two-dimensional surface, S, is assumed to be made up of plane triangular elements, ΔS_i. Although attempts have been made [9] to account for the surface curvature this can only be done approximately and imposes a large burden on the analysis. As important simplifications in the analysis occur by assuming plane surface elements and since many physical problems involve flat surfaces the assumption that the surface is piecewise flat is made. It is further assumed that on each element, ΔS_i, of the surface that the surface data of traction and displacement may be assumed constant. Following

Figure I each surface element is denoted by its centroidal point, Pm or Qn, depending on whether the point is fixed or variable with respect to the integration.
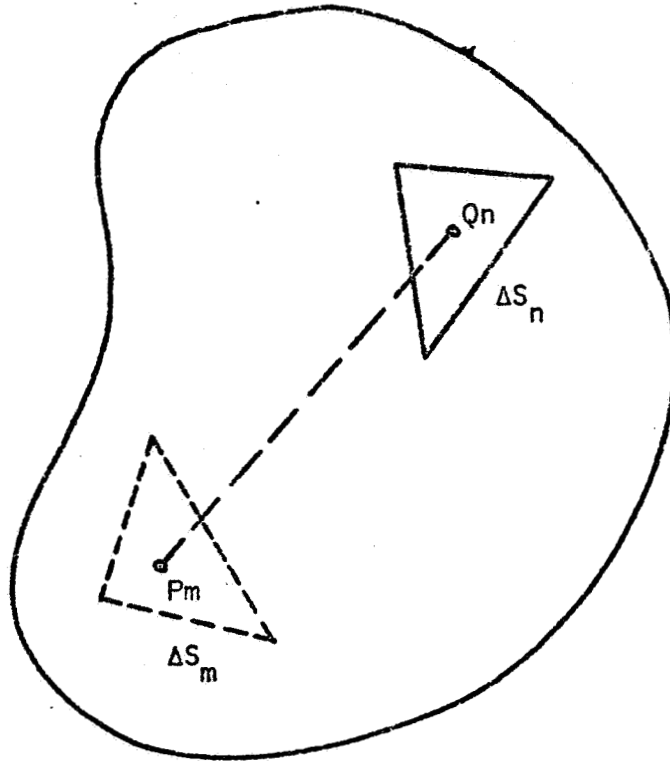

Figure I. Surface Elements

When the surface data is discretized in this way, the integral equations (2.14) may be seen to reduce to the following algebraic equations

$$\frac{1}{2} u_j(Pm) + \sum_n u_i(Qn) \int_{\Delta S_n} T_{ji}(Pm,Q)dS(Q)$$

$$= \sum_n t_i(Qn) \int_{\Delta S_n} U_{ji}(Pm,Q)dS(Q).$$

(3.1)

The values $u_i(Qn)$, $t_i(Qn)$ are now the constant approximations to u_i, t_i on element ΔS_n. The integrals

$$\Delta T_{ij}(Pm,Qn) = \int_{\Delta S_n} T_{ij}(Pm,Q)dS(Q)$$

and   (3.2)

$$\Delta U_{ij}(Pm,Qn) = \int_{\Delta S_n} U_{ij}(Pm,Q)dS(Q)$$

may be calculated automatically to any desired accuracy by knowing the size, orientation and location of ΔS_n and the point Pm. The numerical procedure used for these integrals (3.2) is discussed in Appendix A. Because of the assumption of plane elements it is possible to perform the integrations exactly when Pm = Qn (taking into account the principal value interpretation) and this is detailed in Appendix B. The points Pm and Qn are taken at the centroids of the elements ΔS_n to account best for the variation of u_i and t_i on ΔS_n. Equation (3.1) may now be written as

$$\{\tfrac{1}{2}\delta_{ij}\delta_{mn} + \Delta T_{ij}(m,n)\}u_j(n)$$

(3.3)

$$= \Delta U_{ij}(m,n)t_j(n),$$

which has the matrix representation

$$\{\tfrac{1}{2}[I] + [\Delta T]\}\{u\} = [\Delta U]\{t\}.$$ (3.4)

The matrix $[I]$ is the identity matrix. In general, the solution to the mixed boundary-value problem is obtained by first appropriately rearranging the columns in Eq. (3.4) so that all unknown data appear in the vector $\{x\}$:

$$[A]\{x\} = [B]\{y\}. \tag{3.4}$$

When rearranging, the columns must be scaled to maintain the proper conditioning of matrix $[A]$. This scaling is based on an attempt to keep the diagonal terms in $[A]$ at the same order of magnitude. Equation (3.4) is solved by a standard Gauss reduction scheme on $[A]$ followed by an iteration to refine the solution $\{x\}$. As the matrix $[A]$ is weighted toward the diagonal, it is well conditioned and in actual numerical examples a single iteration usually achieves refinements in $\{x\}$ on the order of $|\{\Delta x/x\}| < .001$. These examples are discussed in the next section.

Finally, after solving Eq. (3.4), the known boundary data may be used to determine the solution for the internal displacements and stresses by direct integration of the identities (2.9) and (2.10). Following the same numerical procedure these are found to be

$$u_j(p) = - \sum_n u_i(Qn)\Delta T_{ji}(Qn,p)$$

$$\tag{3.5}$$

$$+ \sum_n t_i(Qn)\Delta U_{ji}(Qn,p)$$

and

$$\sigma_{ij}(p) = -\sum_n u_k(Qn)\Delta S_{kij}(Qn,p)$$

$$+ \sum_n t_k(Qn)\Delta D_{kij}(Qn,p).$$

(3.6)

The integrations to determine ΔS and ΔD are performed in the same way as those to obtain ΔT and ΔU. Any number of interior solutions may be made once the boundary solution is obtained. Since the solution is performed at pre-selected points the analyst may concentrate on particular areas of interest and is not burdened with complete field solutions. No approximations to the field equations are necessary as all approximations are made at the surface. It can be predicted from St. Venants Principle that the errors are also restricted to near-surface regions. A discussion of these errors is found in the next section.

4. Numerical Results

Some elementary boundary value problems were solved to determine the validity of the approximations discussed in Sec. 3 as well as to investigate the behavior of the numerical procedures under different circumstances. The computed results are for a region with a piecewise flat surface: the cube with unit dimensions. In all cases sufficient boundary displacements are set equal to zero to eliminate the rigid body motion. The surface elements for the unit cube are illustrated in Figure 2 for 12 triangles, in Figure 3 for 24 triangles, and in Figure 4 for 48 triangles. All results have been obtained using a single, general source program written in FORTRAN language. Required data includes the material properties, the surface element arrangement,
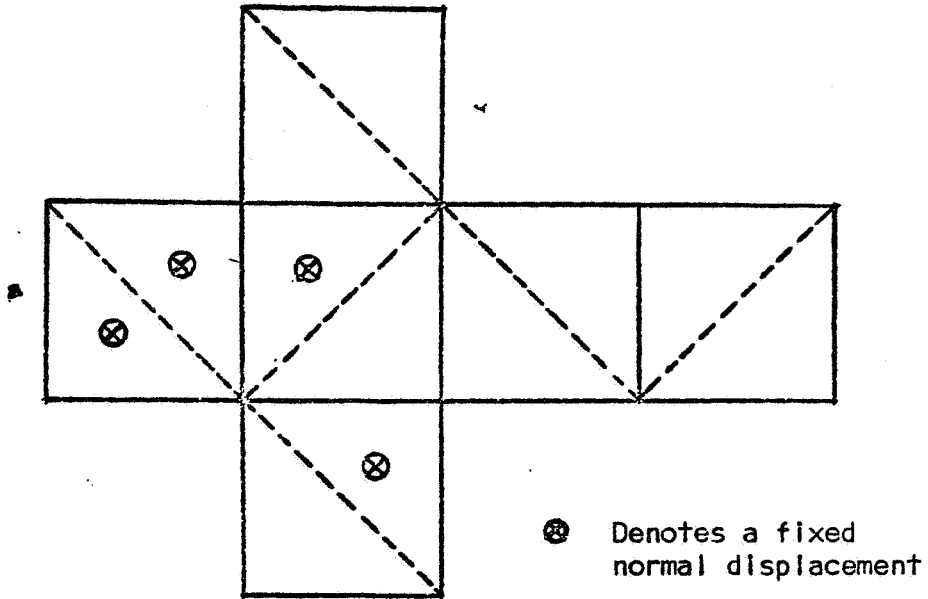
Figure 2.   Unit Cube - 12 Elements

the known surface tractions and displacements which are assumed constant
over each surface element, and the locations of internal points where
the displacements and stresses are desired.

4.1 Uniaxial Stress Distribution

In the first series of problems the unit cube is loaded in a
state of uniaxial tension by the application of a normal stress to
two ends. On one end and on two normal faces the normal displacement
component was set equal to zero. The required tractions at these
elements are then part of the solution. The zero displacements are
indicated on the appropriate cubes in Figures 2, 3 and 4. The
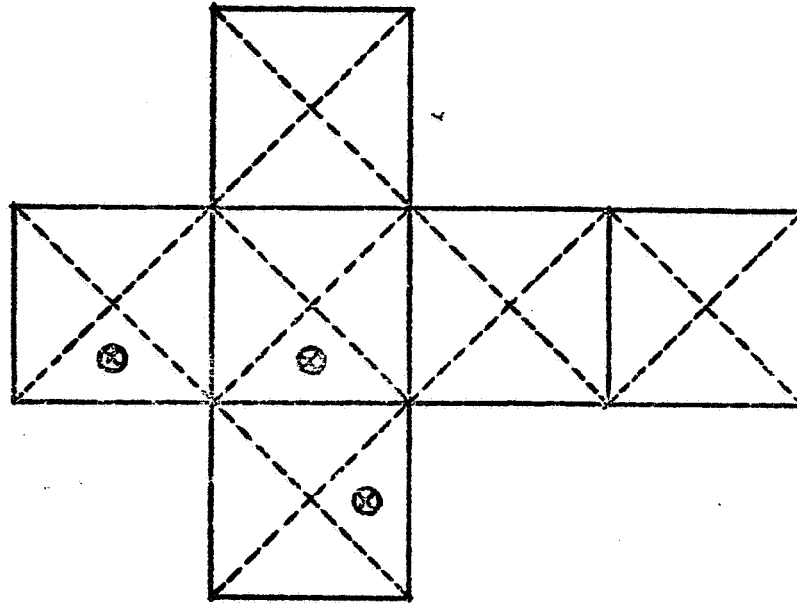surface displacements in the axial and transverse directions are
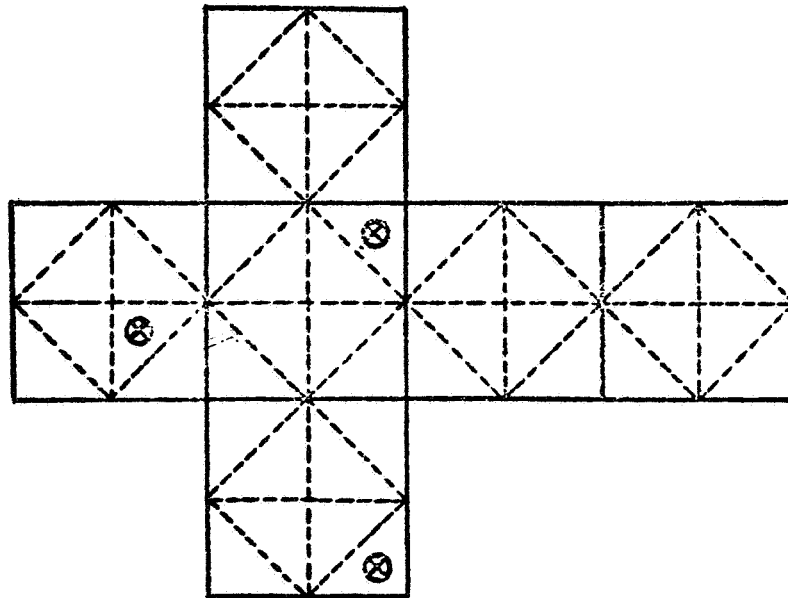
Figure 3.   Unit Cube -- 24 Elements

Figure 4.   Unit Cube - 48 Elements

indicated in Figure 5 for the case of 12 triangles and values of Poisson's ratio varying from zero to one-half. It is obvious from this plot that for values of Poisson's ratio less than one-quarter large errors are found in the transverse displacements. Similar errors can be seen in the two dimensional case [1]. The source of these errors has not yet been determined but it seems that the numerical procedures introduce the error rather than the approximations given in Sec. 3. This is indicated by the fact that no appreciable change is found going to 24 surface elements as shown by the data in Table I for $\nu = 0.25$. The large error is detected only when the transverse displacements are less than the axial displacements by at least an order of magnitude. However, Table I also shows that the calculation of the internal stresses is improved by refining the surface elements and this effect is even more pronounced for lower values of Poisson's ratio.

By assuming the surface displacements at each element to be constant, including the in-plane displacements, the solution method introduces high stresses near the surface. This layer, illustrated for the uniaxial case with 24 elements in Figure 6, is a function only of the size of the surface elements and not the refinement of the integration. Fortunately this layer is restricted to a depth which is a fraction of the size of the element. To determine the stresses at the surface a method is presently being developed which utilizes numerically calculated surface displacement gradients and known tractions as has been demonstrated in [10]. This will enable the analyst to move the interior solution point at will within the region and extend these results to the surface.
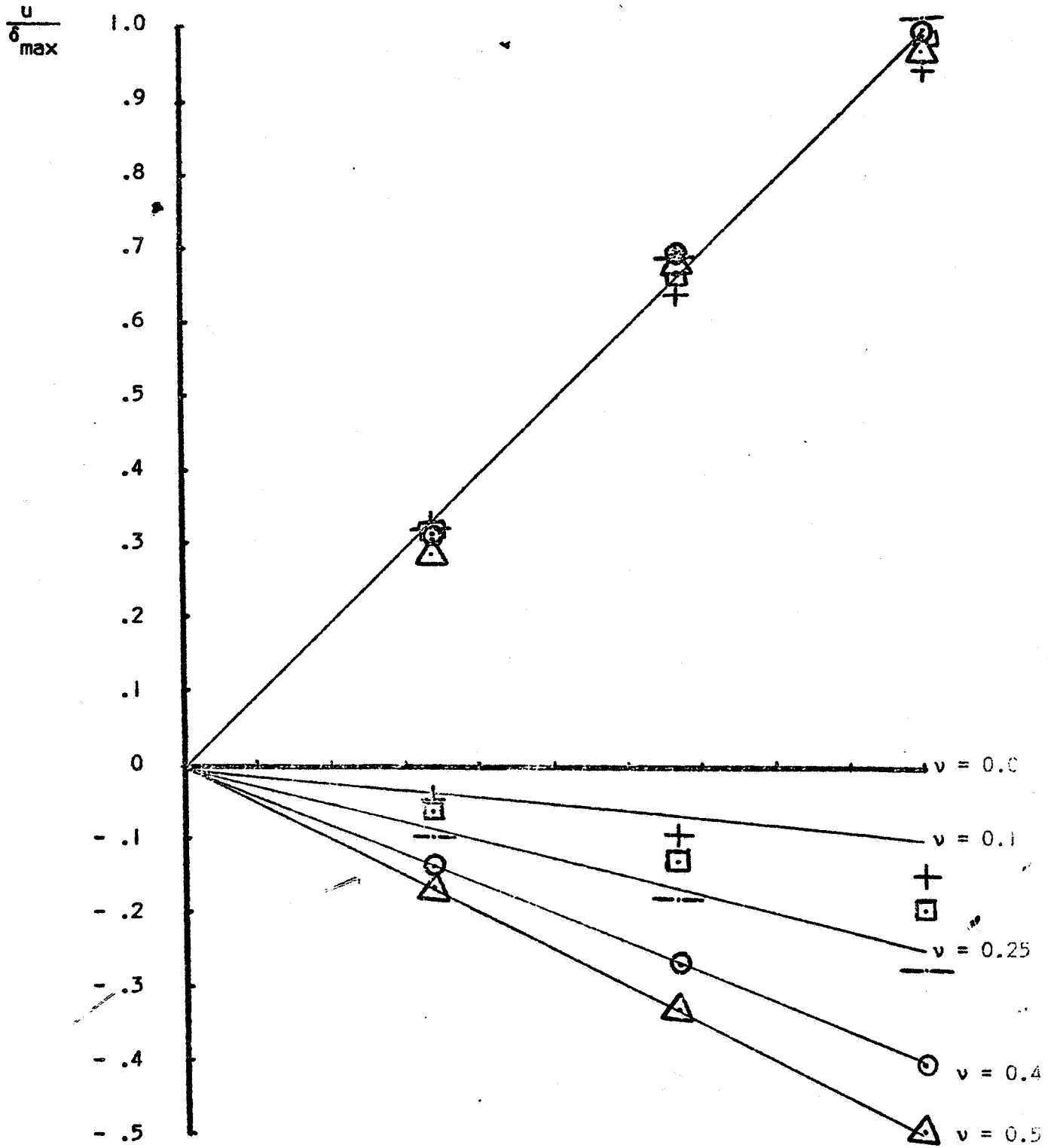
Figure 5. Surface Displacements for Various Poisson's
Ratios, N = 12.

Table 1. Data for the unit cube with 12 and 24 elements under uniaxial tension, p, including surface reactions, surface displacements, and internal stresses at the points (.4, .4, .4) and (.6, .6, .6). Only typical results are shown.

	N = 12	N = 24	Exact
Reactions (t_i/p):	1.0011	1.0012	1.0000
	1.0009		1.0000
	.00059	.00035	.0000
Max. Axial Disp. (u_i/δ):	1.02	1.025	1.000
Max. Trans. Disp.	1.17	1.17	1.000

Internal Stresses:

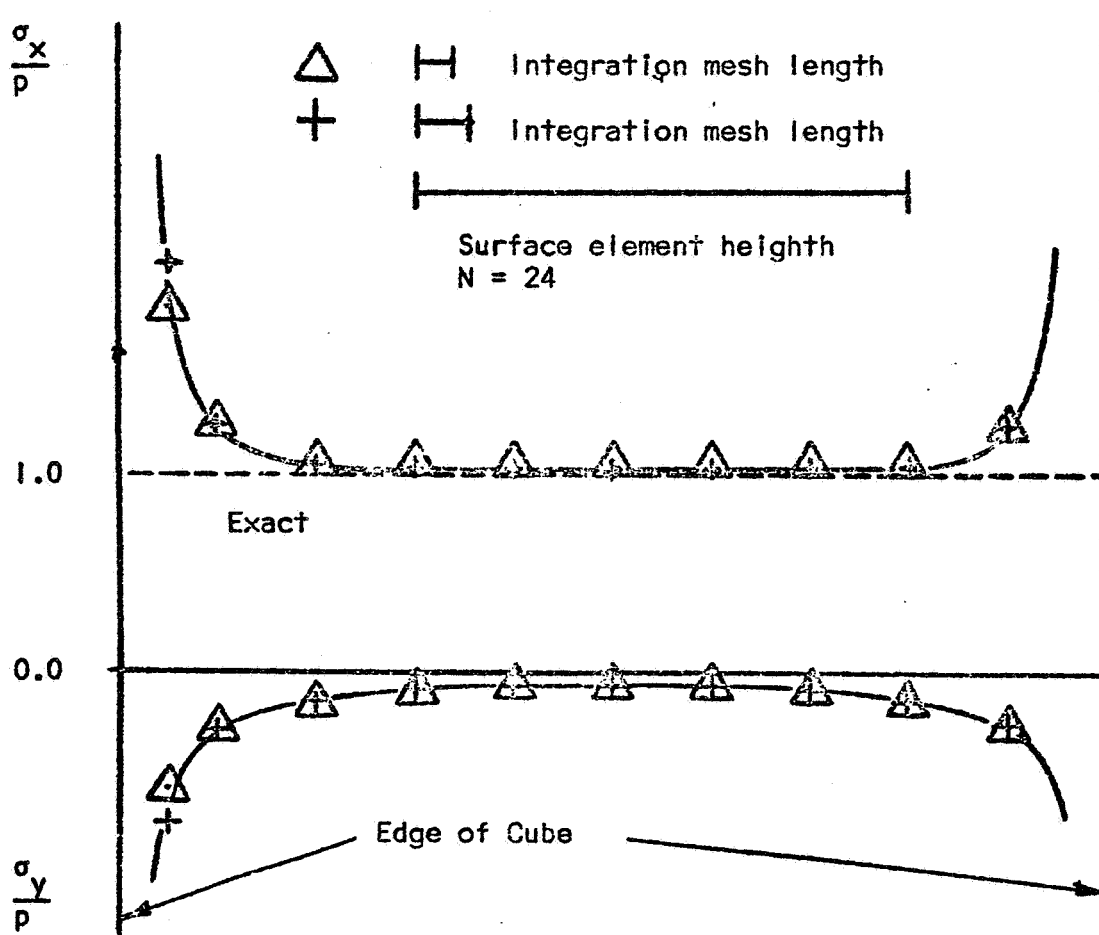|		σ_x/p	σ_y/p	σ_z/p	τ_{xy}/p	τ_{xz}/p	τ_{yz}/p
N = 12	(.4,.4,.4)	1.026	-.05	-.05	.003	.004	-.02
	(.6,.6,.6)	1.027	-.05	-.05	.003	.003	-.01
N = 24	(.4,.4,.4)	1.018	-.08	-.08	-.01	-.01	.02
	(.6,.6,.6)	1.013	-.09	-.09	-.01	.01	-.03
Exact		1.000	.00	.00	.00	.00	.00

Figure 6. Internal Solution - Surface
Layer Error

4.2 Uniform Shear Stress

The second elementary problem was to solve the case of a uniform

shear stress applied to the unit cube in one of its planes. This

problem was solved for the case of 12, 24 and 48 surface elements.

Again, sufficient surface displacements were fixed to zero to eliminate

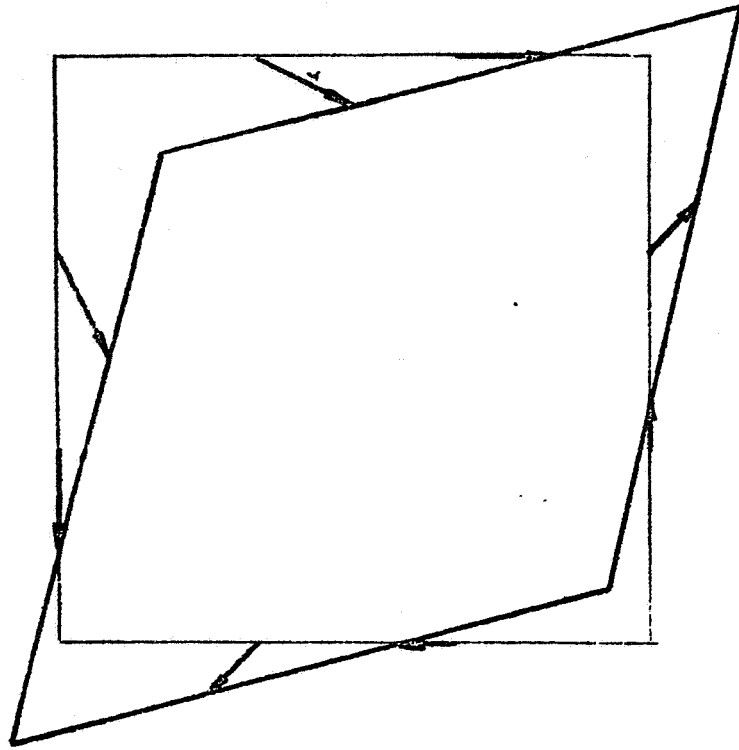rigid body motion. A typical displacement pattern shown for N = 12 is

Figure 7. Surface Element Displacements for Pure Shear, N = 12

given in Figure 7. The numerical results for the non-zero shear strain and the internal stresses are given in Table 2. In this problem the assumption of constant displacement at each element is more constraining than in the previous case and significant improvements are shown for the finer surface meshes.

Table 2. Data for the unit cube loaded in pure shear stress, p, in one of its planes, including computed shear strain and internal stresses for N = 12, 24 and 48.

N	$\gamma\,\gamma_{xz}$	σ_x/p	σ_y/p	σ_z/p	τ_{xy}/p	τ_{xz}/p	τ_{yz}/p	
12	.000726	- .08	- .01	- .06	- .02	.71	- .002	(.4,.4,.4)
		.06	.01	.06	- .04	.69	- .03	(.6,.6,.6)
24	.000795							
48	.000810	- .009	.03	- .009	.02	.95	.02	(.4,.4,.4)
		- .009	.03	.01	.02	.95	.02	(.6,.6,.6)
Exact	.000855	.00	.00	.00	.00	1.00	.00	

It is apparent that although not all questions have been answered the approximations of Sec. 3 are justified for these simple cases. The method is presently being extended to more significant problems but serious difficulties are not expected. The analysis procedure has been completely automated and the analysis has been carried out on a UNIVAC 1108 computer making use of external scratch storage. Run times are not miniscule (about three minutes for the surface solution with 12 elements) but no strong attempt was made to minimize run time.

It is further apparent that very good results can be achieved with a minimum number of elements. When analyzing problems with surface stress concentrations, however, it will be necessary to decrease the element size in that area. Although these examples have all been for equal-sized triangles no numerical difficulty is expected when using various sizes and shapes of elements. It is now envisaged that the procedure described in this document will find wide applicability in inherently difficult problems and that no problems of more than a tactical nature remain.

[1] F. J. Rizzo, *An Integral Equation Approach to Boundary Value Problems of Classical Elastostatics*, Quart. of Appl. Math. 25, April 1967.

[2] T. A. Cruse and F. J. Rizzo, *A Direct Formulation and Numerical Solution of the General Transient Elastodynamic Problem I*, J. Math. Anal. Appl. 22, April 1968.

[3] T. A. Cruse, *A Direct Formulation and Numerical Solution of the General Transient Elastodynamic Problem II*, J. Math. Anal. Appl. 22, May 1968.

[4] O. D. Kellogg, *Foundations of Potential Theory*, Dover, New York, 1953.

[5] R. Courant and D. Hilbert, *Methods of Mathematical Physics Vol. II*, Interscience, New York, 1962.

[6] R. P. Banaugh, *Application of Integral Representations of Displacement Potentials in Elastodynamics*, Bull. Seis. Soc. Amer. 54, August 1964.

[7] A. E. H. Love, *A Treatise on the Mathematical Theory of Elasticity*, Dover, New York, 1944.

[8] L. H. Chen and D. G. Schweikert, *Sound Radiation from an Arbitrary Body*, J. Acous. Soc. Amer. 35, October 1963.

[9] K. M. Mitzner, *Numerical Solution for Transient Scattering from a Hard Surface of Arbitrary Shape - Retarded Potential Technique*, J. Acous. Soc. Amer. 42, August 1967.

[10] F. J. Rizzo and D. J. Shippy, *A Formulation and Solution Procedure for the General Non-homogeneous Elastic Inclusion Problem*, to be published.

Appendix A

Surface Integrals of the Non-Singular Tensors (P ≠ Q)

Since the surface integrations in Eqs. (3.2), (3.5) and (3.6)
cannot, in general, be done in closed form, it is necessary to develop
an automatic procedure which will determine the integrals with sufficient
accuracy in a minimum of time. The method used in this analysis is
similar to that reported in [8], where the kernels correspond to
singular solutions to the Helmholtz equation. The method is based on
an affine transformation which maps any physical surface triangle onto
a basic "unit triangle." The integration is then performed by sub-
dividing the unit triangle and approximating the integral by a finite
sum. The method is suitable for iterating to a desired accuracy but
it was found for this work that the added time of iteration was not
justified. The use of the unit triangle achieves a uniform distribution
of sub-triangles and achieves complete flexibility in the orientation
and shape of the physical triangles.

Assume the body is located in a global coordinate system and that
any point is denoted by its position vector $\vec{p}$. The surface of the
three dimensional body is divided into adjoining, plane triangles,
denoted by some positive integer n. Let the vertices of the triangles
be denoted by the positions $\vec{p}_A$, $\vec{p}_B$ and $\vec{p}_C$ with A, B and C located in a
right-handed sense about the outward pointing normal $\vec{n}$.

The numerical integration of the kernels T, U, S and D when
P ≠ Q is accomplished by first mapping the physical triangle onto a
unit triangle. The unit triangle is indicated in Figure 2. The point
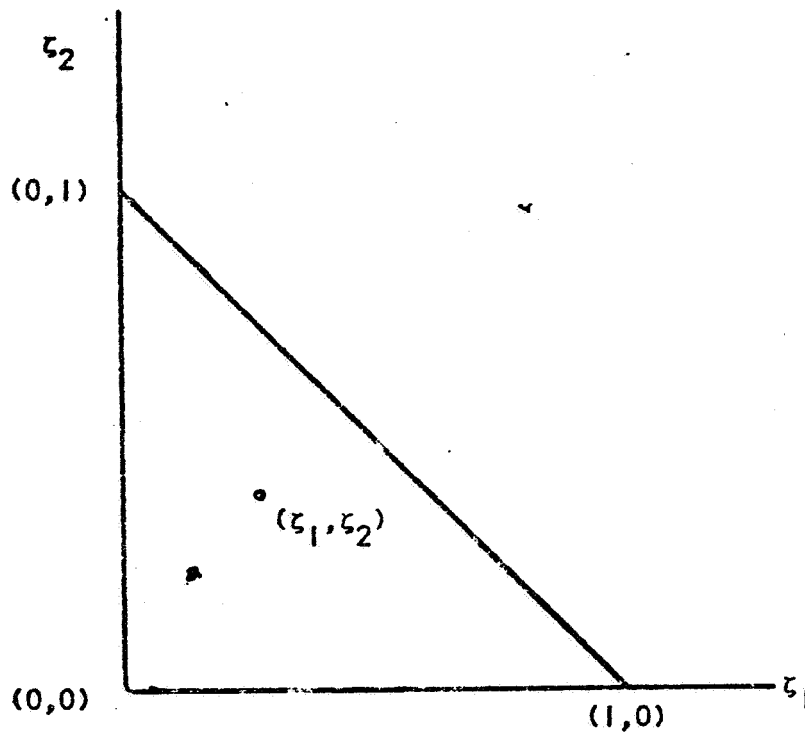(0,0) is chosen to correspond to corner A, (1,0) to corner B, and

Figure A-1. The Unit Triangle

(0,1) to corner C. Corner A should be the largest corner for the best conditioning of the procedure. Let the point (ζ_1, ζ_2) correspond to the variable point Q and let this be located relative to the corner A in the following way:

$$\vec{\rho}_Q = \vec{\rho}_A + \zeta_1(\vec{\rho}_B - \vec{\rho}_A) + \zeta_2(\vec{\rho}_C - \vec{\rho}_A). \tag{A.1}$$

The numerical integration is accomplished by first dividing the unit triangle into M equal elements (see Figure A-2 for M = 4) and calculating the locations of the centroids of the sub-element triangles by the procedure given in the following FORTRAN instructions:
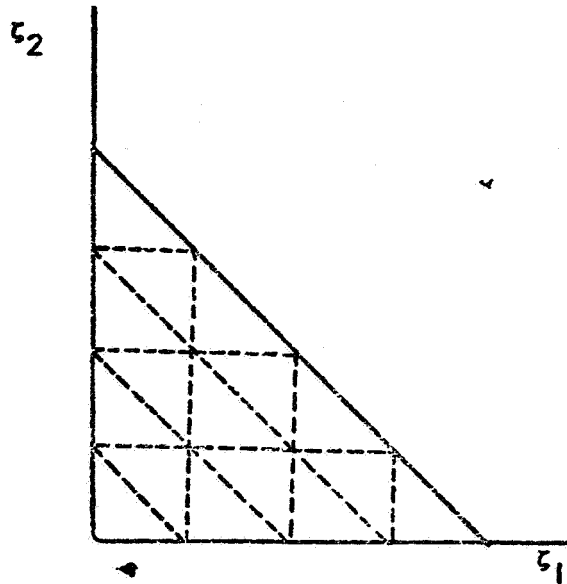
Figure 4-2. Division of the Unit Triangle, M = 4

```
NFINAL = 2*M - 1

DO 60  J = 1, NFINAL, 2

DO 60  I = 1, J, 2

LIM = 1

IF  (I .EQ. J)  LIM = 2

DO 60  K = LIM, 2

ZETA1  =  (I*0.5 + .166667*(-1)**K)/M

ZETA2  =  1.0 - (J*0.5 + .166667*(-1)**(K+1))/M

IF  (I .NE. J)  GØTØ 60

ZETA1  =  (I*0.5 - .166667)/M

ZETA2  =  1.0 - (J*0.5 + .166667)/M

60    CØNTINUE
```

For each point (ξ_1,ξ_2) Eq. (A.1) determines a point Q for which the integrand can be calculated. The value of the integral is approximated by assuming constant values of the kernels over each sub-element,

evaluating the integrand, and by adding the terms for each sub-element. The results can be improved by increasing the value of M until some level of accuracy has been achieved.

Appendix B

Integration of the Singular Tensors (P = Q)

When the fixed point P and the field point Q are in the same triangles, the kernels U_{ij} and T_{ij} contain singularities of the order $1/r(P,Q)$ and $(1/r(P,Q))^2$, respectively. These integrals are to be interpreted in the sense of the Cauchy Principal Value in that the region very close to the point P is excluded from the integral and the integral is to be evaluated as that region shrinks to zero. By letting the surface be represented by plane elements it is possible to perform these integrals exactly.

1. Exact Integration of U_{ij}

The integral to be evaluated is given in Eq. (3.2) as

$$\Delta U_{ij}(Pm, Qn) = \int_{\Delta S_n} U_{ij}(Pm, Q) dS(Q) \tag{B.1}$$

where

$$U_{ij} = \frac{1}{4\pi\mu} \left(\frac{1}{r}\right) \left\{ \frac{3 - 4\nu}{4(1 - \nu)} \delta_{ij} + \frac{1}{4(1 - \nu)} r_{,i} r_{,j} \right\}. \tag{B.2}$$

Let $dS(Q) = r\,dr\,d\theta$ and perform the integration using polar coordinates. Let $r = r(\theta)$, then Eq. (B.1) becomes for $Pm = Qn$

$$\Delta U_{ij} = \lim_{\rho \to 0} \left\{ \frac{1}{4\pi\mu} \int_0^{2\pi} \left[(r(\theta) - \rho)\left(\frac{3 - 4\nu}{4(1 - \nu)} \delta_{ij} + \frac{1}{4(1 - \nu)} r_{,i} r_{,j}\right) \right] d\theta \right\}$$

$$\tag{B.3}$$

which becomes

$$\Delta U_{ij} = \frac{1}{4\pi\mu} \int_0^{2\pi} r(\theta)\left[\frac{3 - 4\nu}{4(1 - \nu)} \delta_{ij} + \frac{1}{4(1 - \nu)} r_{,i} r_{,j}\right] d\theta. \qquad (B.4)$$

Now let the triangle be located in a local coordinate system as shown in Figure B-1. Let side 1-2 be parallel to the ζ_1 axis and investigate the integral of Eq. (B.4) from θ_1 to θ_2 first.
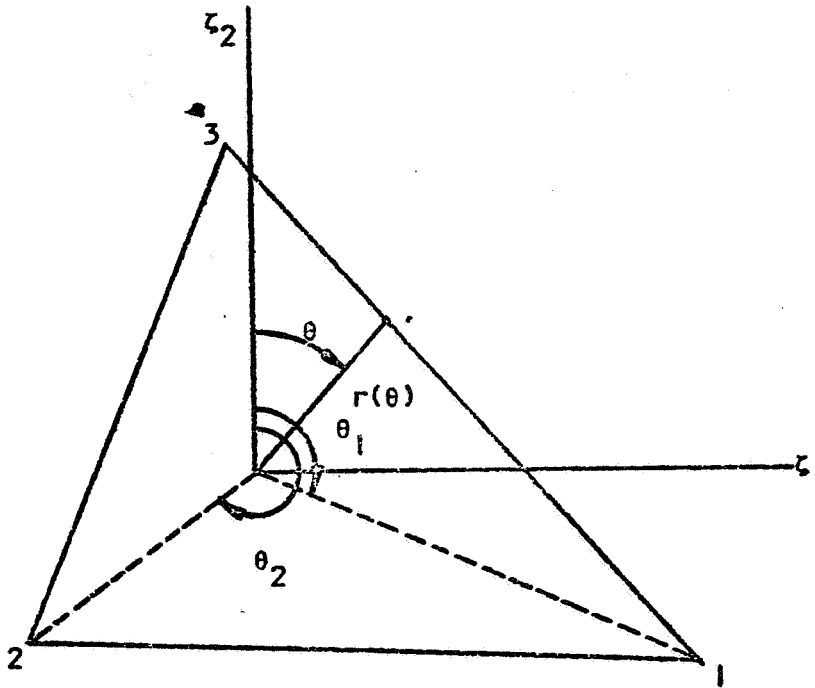

Figure B-1. Geometry of Integration – ΔU

Let the following changes in variables be made:

$$\frac{\partial r}{\partial x_i} = \frac{\partial r}{\partial \zeta_1} \frac{\partial \zeta_1}{\partial x_i} + \frac{\partial r}{\partial \zeta_2} \frac{\partial \zeta_2}{\partial x_i} \qquad (B.5)$$

where

$$\frac{\partial r}{\partial \zeta_1} = \sin\theta, \quad \frac{\partial r}{\partial \zeta_2} = \cos\theta.$$

The terms $\frac{\partial \zeta_{1,2}}{\partial x_i}$ are the direction cosines of the ζ_1 and ζ_2 axes. If base vectors $\vec{e}_1$ and $\vec{e}_2$ are defined for the ζ_1 and ζ_2 axes and the components of these base vectors in the global coordinate system are denoted by e_{1i} and e_{2i} then

$$r_{,i}r_{,j} = \sin^2\theta e_{1i}e_{1j} + \cos^2\theta e_{2i}e_{2j}$$

$$+ \sin\theta\cos\theta(e_{1i}e_{2j} + e_{2i}e_{1j}). \qquad (B.6)$$

Along 1-2 $r\cos\theta = c_1$

or $r(\theta) = c_1/\cos\theta.$ $\qquad (B.7)$

With these substitutions the integral from θ_1 to θ_2 becomes

$$\Delta U_{ij}\Big|_{\theta_1}^{\theta_2} = \frac{c_1}{4\pi\mu} \left\{ \frac{3 - 4\nu}{4(1 - \nu)} \delta_{ij}[\log(\tan\theta + 1/\cos\theta)] \right.$$

$$+ \frac{1}{4(1 - \nu)} [e_{1i}e_{1j}(-\sin\theta + \log(\tan\theta + 1/\cos\theta))$$

$$+ e_{2i}e_{2j}\sin\theta - (e_{1i}e_{2j} + e_{2i}e_{1j})\cos\theta]\Big\}\Big|_{\theta_1}^{\theta_2}. \qquad (B.8)$$

The entire integral may now be calculated by reorienting the ζ_1 and ζ_2 axes so that the ζ_1 axis is parallel to side 2-3 and then parallel to side 3-1. The results are easily obtained in terms of the coordinates of P and the corners, 1,2 and 3.

2. Exact Integration of T_{ij}

The integral to be evaluated in this case is also given in Eq. (3.2):

$$\Delta T_{ij}(Pm,Qn) = \int_{\Delta S_n} T_{ij}(Pm,Q)dS(Q), \tag{B.9}$$

where, for a plane surface (i.e., $\partial r/\partial n = 0$), the kernel T_{ij} is given by

$$T_{ij} = \frac{k}{4\pi} (\frac{1}{r^2})(n_j r_{,i} - n_i r_{,j}). \tag{B.10}$$

By substituting

$$\varepsilon_{ijk}\varepsilon_{rsk}n_r(\frac{1}{r})_{,s} = \frac{1}{r^2}(n_j r_{,i} - n_i r_{,j}) \tag{B.11}$$

into Eq. (B.10) the integral becomes

$$\Delta T_{ij} = \frac{k}{4\pi} \varepsilon_{ijk} \int_{\Delta S} \varepsilon_{rsk}n_r(\frac{1}{r})_{,s} dS. \tag{B.12}$$

The integrand is the k-th component of

$$\vec{n} \times \nabla(1/r)$$

so that by using Stokes' theorem the area integral is converted into the path integral:

$$\Delta T_{ij} = \frac{k}{4\pi} \epsilon_{ijk} \oint \frac{1}{r} dx_k. \qquad (B.13)$$

Because of the principal value interpretation of this integral the path must also exclude the region near P (see Figure B-2). Let C denote the path around the edge of the triangle and C* the circular path of radius ϵ around the point P. Then it follows that
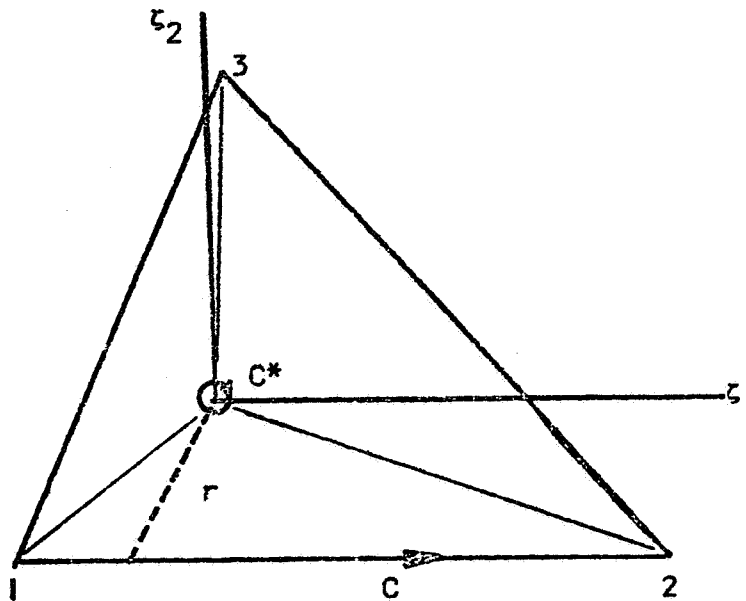

Figure B-2. Geometry of Integration - ΔT

$$\oint_{C^*} \frac{1}{r} dx_k = \frac{1}{\epsilon} \oint_{C^*} dx_k = 0. \qquad (B.14)$$

Again change the variables to a local coordinate system such that

$$dx_k = a_{k1} d\zeta_1 + a_{k2} d\zeta_2 \qquad (B.15)$$

where a_{k1} and a_{k2} are the direction cosines of the ζ_1 and ζ_2 axes. As in the previous section these are the components of the unit base vectors:

$$e_{11} = a_{11}, \quad e_{21} = a_{12}. \qquad (B.16)$$

Let the side 1-2 be parallel to the ζ_1 axis and integrate this side first. Then, since $r = (\zeta_1^2 + \zeta_2^2)^{1/2}$, and $dx_k = e_{1k}d\zeta_1$

$$\Delta T_{ij}\Big|_1^2 = \frac{k}{4\pi}\, \varepsilon_{ijk} \int_1^2 \frac{e_{1k}d\zeta_1}{\sqrt{\zeta_1^2 + \zeta_2^2}}$$

$$= \frac{k}{4\pi}\, \varepsilon_{ijk} e_{1k} \big[\log(\zeta_1 + r)\big]\Big|_1^2. \qquad (B.17)$$

In the same way as before, this integral may be completed by letting the ζ_1 axis be parallel to the 2-3 side and the 3-1 side. This integral may also be automatically computed knowing the locations of the corners and the point P.